ELSEVIER

Journal of Molecular Catalysis A: Chemical 167 (2001) 141–155

JOURNAL OF MOLECULAR CATALYSIS A: CHEMICAL

www.elsevier.com/locate/molcata

Everett's sorption hysteresis domain theory revisited from the point of view of the dual site-bond model of disordered media

Fernando Rojas [a,b,*], Isaac Kornhauser [a], Carlos Felipe [a], Salomón Cordero [a]

[a] *Departamento de Química, Universidad Autónoma Metropolitana-Iztapalapa, P.O. Box 55-534, México 09340, D.F., Mexico*

[b] *Laboratorio de Física Aplicada y Tecnología Avanzada, Instituto de Física, Universidad Nacional Autónoma de México, P.O. Box 1-1010, Querétaro 76000, Qro., Mexico*

Received 5 April 2000

Abstract

The classical and elegant independent sorption domain theory introduced by Everett marked a milestone in the field of adsorption, since it allowed via their famous complexion diagrams a straightforward visualization of the state of individual pores, i.e. filled or emptied of condensate according to their sizes, of an adsorbent in contact with a vapor. The principal results of the independent domain theory are comprised in a series of theorems. The applicability of these theorems is now examined from the point of view of the dual site-bond model, a non-independent pore domain approach that has been proved to be very useful to simulate porous networks and capillary phenomena occurring wherein. © 2001 Elsevier Science B.V. All rights reserved.

Keywords: Sorption hysteresis; Independent sorption domain theory; Dual site-bond model

1. Introduction

Everett's *independent domain theory of sorption hysteresis* (*ISDT*) first saw the light between 1952 and 1955 in a series of publications in the transactions of the Faraday society [1–4]. The main assumption of the theory consisted in visualizing the porous network as an assemblage of independent pores, whose behavior during the capillary process not depended on each other. Every pore domain was characterized by two quantities; each indicating, respectively, the critical conditions at which the vapor → liquid and the liquid → vapor irreversible transitions there occurred. Hysteresis was then recognized at the level of one pore and brought about to the level of the whole network, through the summation of individual pore hysteretic contributions. Among the results provided by the *ISDT* two are very important: (1) the state of each pore entity can be visualized through a *domain complexion diagram*, a graph in which every pore domain is identified as either full or empty of capillary condensate according to its size; (2) the shapes and qualitative behavior of scanning curves or subsidiary cycles within the main hysteresis loop can be inferred from a series of theorems.

In spite of the success of the *ISDT* in explaining several experimental sorption facts, Everett himself [5] pointed out that a more general theory of sorption hysteresis should be necessary in order to improve the agreement between experimental and theoretical expectations found so far through the *ISDT*. Thus, it would be essential to consider the appropriate cor-

* Corresponding author.
E-mail address: fernando@xanum.uam.mx (F. Rojas).

1381-1169/01/$ – see front matter © 2001 Elsevier Science B.V. All rights reserved.
PII: S1381-1169(00)00501-X

relations that arise among the voids of an interconnected porous network in order to adequately interpret or simulate a given sorption process. An approach of such a kind would constitute a non-independent domain theory. The *dual site-bond model* (*DSBM*) of complex media allows the construction of topologically heterogeneous porous networks, based on the recognition of two basic void elements that constitute the substrate: the *sites* (cavities) and the *bonds* (throats, capillaries). The heterogeneity of a porous network can be ascribed to the following properties:

1. pores can adopt different sizes according to a preestablished twofold distribution of sites and bonds [6,7],
2. the connectivity, that is the number of neighbors to which a pore cavity is interconnected, can vary from one site to another [8],
3. there may arise geometrical restrictions among bonds [9], in the sense that there should exist no interpenetration between any pair of pore channels before reaching the cavity to which both bonds are being connected.

This work gives emphasis to the ascertainment or not of the theorems advanced by the *ISDT*, with respect to sorption processes occurring in non-independent pore domain systems. First, some basic notions concerning the main characteristics of a typical sorption isotherm and some of the different processes developed within its hysteresis loop will be outlined. Second, a general overview of the *ISDT* and its incumbent theorems will be presented. Third, fundamentals of the *DSBM* and analytical expressions of some sorption processes occurring in such a substrate will be provided in order to realize the type of particularities involved during pore filling with a given fluid. Finally, the results supplied by the *DSBM* with respect to the validity or contravention of the theorems of the *ISDT* approach about sorption phenomena taking place in non-independent pore domains will be discussed. This discussion will be made for the case of selected porous networks with a minimal number of constraints. Monte Carlo sorption simulations will be employed to determine the sorption curves and sometimes, when possible, analytical expressions will be used to describe a particular sorption process.

2. Theory

2.1. Basic aspects [5]

An adsorption isotherm of a vapor on an adsorbent solid surface (in which the amount of gas adsorbed is plotted against the relative vapor pressure $x \equiv p/p^0$ of the adsorptive, p being the vapor pressure and p^0 the saturation vapor pressure at temperature T) exhibits several characteristics (see Fig. 1). Usually, the isotherm displays a *hysteresis loop* (*HL*) delimited by the *boundary ascending* (*BA*) *curve* and the *boundary descending* (*BD*) *curve*. The lowest value of x that corresponds to the onset of the hysteresis phenomenon is known as the *inception point*, whilst the highest x point at which the loop closes is the *closure point*, at these two points both the *BA* and the *BD* curves coincide. An infinite number of different trajectories can be drawn within the hysteresis loop; all these correspond to scanning processes. A *primary scanning ascending* process (*PA*) consists in an adsorption path starting at some point on the *BD* curve (the *point of reversal or inversion*) that finishes at some intermediate point within the *HL*, the scanning process concludes when the *BA* curve is reached. A *primary scanning descending* curve (*PD*) consists in a desorption process started at some point of the *BA* curve (point of reversal) and continued down to some point in the *HL*, here again the scanning process ends if the *BD* curve is reached.

The critical conditions for condensation or evaporation of a substance to take place in individual pores can be predicted by means of the Kelvin equation:

$$RT \ln \frac{p}{p^0} = \sigma^{\mathrm{lg}} v^{\mathrm{l}} C^{\mathrm{lg}} \tag{1}$$

where σ^{lg} is the surface tension of the liquid–gas interface, v^{l} the molar volume of the adsorptive, C^{lg} the curvature of the liquid–gas interface, R the gas constant and T the absolute temperature. C^{lg} is related to R_{c}, the mean critical radius of curvature of the liquid–gas interface through the equation $C^{\mathrm{lg}} = 2/R_{\mathrm{c}}$. The different menisci geometries that arise when condensation or evaporation processes take place, are the causes of the hysteresis observed at the level of a single pore [10]. Neglecting the influence of the adsorbed layer, a spherical pore of radius R_{sp} will become filled with condensate when the radius of curvature of the interface appearing inside the void

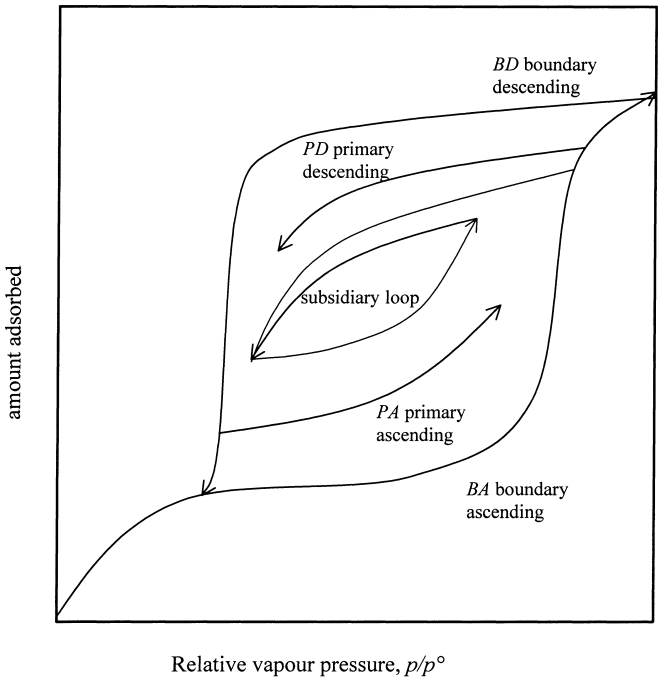

Fig. 1. Sorption isotherm showing the main hysteresis loop (*HL*), the boundary ascending (*BA*) curve, the boundary descending (*BD*) curve, a primary ascending (*PA*) curve, a primary descending (*PD*) curve and a subsidiary loop.

is equal to the pore radius ($R_c = R_{sp}$). In turn a cylindrical capillary will become filled with liquid if the interface has a radius of curvature twice as that of the cylinder ($R_c = 2R_{cyl}$). Evaporation of condensate from a cylindrical pore occurs when $R_c = R_{cyl}$.

2.2. Fundamentals of the domain theory of sorption hysteresis [1–5]

Sorption hysteresis in porous media can be analyzed on the basis of Everett's *ISDT*. In this treatment, individual sorption pore hysteresis properties (related to the conditions required for an isolated pore entity to be fully invaded by a certain fluid) manifest together during the occurrence of the capillary process and help explaining the sorption hysteresis phenomenon observed at the level of the whole substrate.

In this work, the porous structure is envisaged as a collection of independent or isolated *pore domains*. Citing Everett [5], a pore domain is a region of pore space accessible from neighboring regions through pore constrictions. In the simple case of the pore space formed by equal spheres in hexagonal close packing, the pore domains may be identified with the tetrahedral and octahedral cavities (sites, antræ), which are joined through windows (constrictions, necks) with the shapes of triangular foramina. An isolated pore domain have well-defined condensation–evaporation characteristics involving one or more spontaneous irreversible steps.

Each pore domain can be characterized by two relative vapor pressure values, x_{12} and x_{21}, that indicate the onsets at which irreversible condensation or evaporation phenomena take place, respectively. The quantity x_{12} represents the relative pressure required for a pore domain to be filled with capillary condensate, by displacing the vapor phase that was originally occupying the cavity. The quantity x_{21} represents, in turn, the conditions required for the liquid–gas interface to sweep throughout the cavity removing the liquid-like phase while substituting it with vapor.

For adsorption–desorption processes occurring within an isolated pore domain, it is always found that $x_{12} \geq x_{21}$, therefore, the reason of *pore hysteresis*.

This inequality can be visualized graphically via a diagram in which pore domains are located inside the limits of an equilateral triangle of base x_{12} and height x_{21}. Reversible adsorption–desorption properties may sometimes arise (e.g. a cylindrical pore open at one end and closed at the other, can be liquid-filled and liquid-emptied reversibly) and are located around the hypotenuse of the triangle. Associated to each element of area in this triangular diagram, there exists a quantity $v(x_{12}, x_{21})$ such that $v(x_{12}, x_{21})\,\mathrm{d}x_{12}\,\mathrm{d}x_{21}$ represents the volume of the pore domains contained between $(x_{12}, x_{12}+\mathrm{d}x_{12})$ and $(x_{21}, x_{21}+\mathrm{d}x_{21})$. Thus, the volume density distribution function $v(x_{12}, x_{21})$ characterizes the properties of the pore domain.

2.3. The ISDT

The foundation of this theory consists in imagining that the porous medium is made of a collection of individual non-interacting pore domains (e.g. an arrangement of parallel non-intersecting capillary tubes). Therefore, individual domain volumes $v(x_{12}, x_{21})\,\mathrm{d}x_{12}\,\mathrm{d}x_{21}$ can be added together to build an overall distribution function embodying the distribution condensation–evaporation properties of the whole adsorption system.

If the values of $v(x_{12}, x_{21})$ are plotted vertically to the triangular base of the plane x_{12}, x_{21}, then a surface appears over this plane. The volume comprised between this surface and the triangular base from $x_{12} =$ 0–1 represents the total porous space, V^{p}:

$$V^{\mathrm{p}} = \int_0^1 \int_0^{x_{12}} v(x_{12}, x_{21})\,\mathrm{d}x_{21}\,\mathrm{d}x_{12} \tag{2}$$

When a certain state of the adsorption process in the porous substrate is reached, the volume V of all pore domains filled with condensate (having started with an empty pore system at zero pressure) at a relative vapor pressure x_{12} is given by

$$V = \int_0^x \int_0^{x_{12}} v(x_{12}, x_{21})\,\mathrm{d}x_{21}\,\mathrm{d}x_{12} \tag{3}$$

Graphically, a *BA* process of this kind can be represented by the movement of a vertical line from left ($x = 0$) to right (x_{12}) across the triangular base (Fig. 2c). A diagram representing this and other types of sorption processes has been called a *domain complexion diagram*. In this type of diagram, the extents of liquid- and vapor-filled elements can be appreciated while distinguished from each other. A complexion diagram is a plot depicting the pore size distribution function below which there are lines that delimit blank areas (vapor) from black-areas (condensate) (Fig. 2a and c, $F(R)$ representing the pore size distribution function).

A *BD* process can be visualized through the movement of a horizontal line from top to bottom of a complexion diagram. Having all pores initially filled with condensate ($x = 1$) and if then the relative pressure is decreased to some value x, this desorption process will cause that some pore domains be now emptied of condensate. The volume of liquid V remaining inside the pore domains after the desorption process has taken place from $x = 1$ to x is (Fig. 2a′ and c′):

$$V = V^{\mathrm{p}} - \int_x^1 \int_x^{x_{12}} v(x_{12}, x_{21})\,\mathrm{d}x_{21}\,\mathrm{d}x_{12} \tag{4}$$

A *PD* curve consists of a desorption process originated at an upper relative pressure x_{ui} (i.e. the point of inversion) on the *BA* curve down to a lower relative pressure x_{l} in the hysteresis cycle. The corresponding domain complexion diagram of a particular state reached through a *PD* curve can be obtained by the movement of a vertical line from $x = 0$ to x_{ui} followed by the displacement of a horizontal line from x_{ui} to x.

A *PA* curve consists of an adsorption process initiated at the lower point of inversion x_{li} located on the *BD* curve, followed by an adsorption process from this state to an upper point x_{u} lying somewhere within the hysteresis loop. Construction of the domain complexion diagram involves the movement of a vertical line from the point of inversion x_{li} to the upper limit x_{u} of the *PA* curve.

2.3.1. Theorems stated by the ISDT

These are the theorems advanced by the *ISDT*:

Theorem 1. *If the PD curve from x_u meets the BD at x_l, then the PA curve from x_l meets the BA at x_u.*

Theorem 2. *If all the PD curves converge on the lower inception point of the HL, all the PA curves will converge on the upper closure point.*

Theorem 3a. *The slope of any scanning curve (SC) is zero at the point of reversal.*

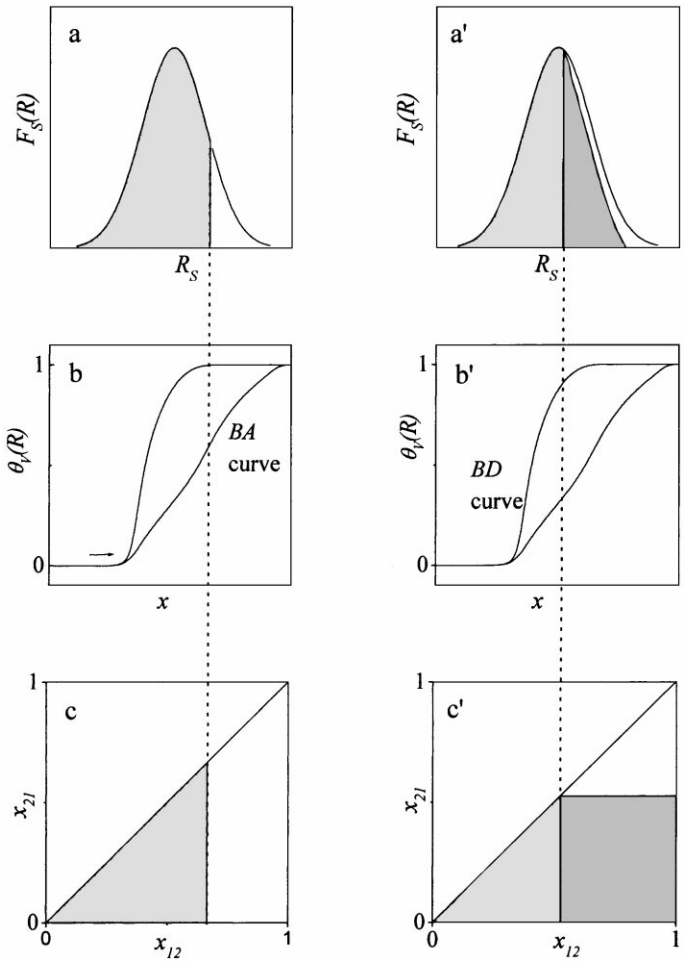

Fig. 2. Domain complexion diagrams for a *BA* curve (at left) and a *BD* curve (at right), at certain stages of the corresponding sorption process. Black and gray areas represent pores filled with condensate, blank areas correspond to vapor-filled pores. (a, a′) Domain complexion diagrams; (b, b′) sorption curves; (c, c′) triangular diagrams. Areas in gray correspond to blocked pores during the descending process.

Theorem 3b. *The slope of any SC at a given value of x is less than the slope at the same value of x of all curves of lower order into which it runs, when, for an ascending curve, x is increased, or for a descending curve x is decreased.*

Theorem 4. *If the path of the system is reversed at A* ($x = x_A$) *and x is changed to* x_B *and back to* x_A*, then the system will return to A. Any oscillation of x between the given limits* x_A *and* x_B *will lead to a loop of constant shape and area independent of the position of A in the loop.*

Theorem 5. *If, when the system returns to A as envisaged in Theorem 4, x continues to increase, the system will move along the same curve as that which would have been followed if no loop had been traversed from A.*

Theorem 6. *Any point P within the HL can be reached in an infinite number of ways, some from lower values of x, some from higher. The system will have definite static macroscopic properties at this point, but its state will not be completely defined since its behavior when it moves away from*

P depends on the route by which this point was approached.

Theorem 7. *If a system is taken through a series of oscillations of x of decreasing amplitude, after the nth reversal the system moves towards the point at which the* $(n-1)$*th reversal occurred, if the system is carried through this point it moves towards the* $(n-3)$*th reversal point and so on.*

2.4. DSBM of disordered media

As stated by Everett, the predictions provided by the *ISDT* are, in general, fulfilled qualitatively when considering the areas of the x_{12}, x_{21} plane over which integrations are performed to visualize the amount of pores filled with condensate during a sorption process. However, those predictions that involve actual values of the volume integrals are of less general validity ([5], p. 1100). An additional inconvenient is that the independent domain theory has failed to account for all the experimental observations and a non-independent domain theory is thus required.

The *DSBM* of disordered media conceived by Mayagoitia is especially convenient to perform a proper modeling of porous structures [6–9]. Before starting the study of any capillary process in a porous medium, a proper idea of the topology of the substrate should be borne in mind. An adequate model will help to identify possible pore interactions occurring during a capillary process and that the *ISDT* cannot envisage.

The principal characteristics of the *DSBM* are as follows. The porous solid is modeled as an interconnected network of two kinds of alternated voids: *site*s (cavities) and *bonds* (necks, windows). Every site is connected to C neighboring sites by bonds; each bond is the link between two sites (C denotes the *connectivity* of the network). C can vary from site to site, for simplicity it will be assumed here as constant and so in this work the network will resemble a regular lattice.

The theory establishes that instead of considering only the size distribution of voids without paying attention to the kind of element (site or bond) to which the pores belong (as it has been traditionally done), it would be more appropriate to consider a two-fold distribution of sizes. In this way, $F_S(R)$ and $F_B(R)$ are defined as the normalized size distribution functions (on a number of elements basis) of sites and bonds, so that the probabilities to find a site, $S(R)$, or a bond, $B(R)$, having a size R or smaller are, respectively:

$$S(R) = \int_0^R F_S(R)\,\mathrm{d}R;$$
$$B(R) = \int_0^R F_B(R)\,\mathrm{d}R \tag{5}$$

An important parameter of the two-fold distribution of sites and bonds is the degree of overlapping Ω between $F_S(R)$ and $F_B(R)$, i.e. the common area shared between the two distributions. Ω is a measure of the size correlation existing among pore entities.

A *construction principle* (*CP*) emerges from the very definitions of site and bond: the size of any bond should be always smaller than or at most equal to the size of the site to which it is linked. Two self-consistency laws guarantee the fulfillment of the *CP*. The first law establishes that bonds must be sufficiently small and supplied in such a number as to be accommodated together with all the sites belonging to a given size distribution.

A second law is still required since when Ω is considerable, there may appear topological size correlations between neighboring pore elements. Therefore, the joint event of finding a site of size R_S linked to a bond of size R_B is not independent and the probability density for this to occur is

$$\rho(R_S \cap R_B) = F_S(R_S)F_B(R_B)\phi(R_S, R_B) \tag{6}$$

The second law can be expressed as

$$\phi(R_S, R_B) = 0 \quad \text{for } R_S < R_B \tag{7}$$

If the randomness in the topological assignation of sizes is raised up to a maximum, while complying with the *CP*, the most *verisimilar* (likely) form of ϕ for the correct case $R_S \geq R_B$ is obtained:

$$\phi(R_S, R_B) = \frac{\exp\left(-\int_{S(R_B)}^{S(R_S)} \mathrm{d}S/(B-S)\right)}{B(R_S) - S(R_S)}$$
$$= \frac{\exp\left(-\int_{B(R_B)}^{B(R_S)} \mathrm{d}B/(B-S)\right)}{B(R_B) - S(R_B)} \tag{8}$$

These topological size correlationships promote a *size segregation effect*, consisting in that sites and bonds of the bigger sizes join together to form regions of large elements, while elements of the smaller

sizes reunite to constitute alternated regions of small entities. This effect becomes more important as Ω increases. The consequences of this effect on the development of capillary processes are of the utmost importance.

The *CP* can be extended or reformulated to allow for more constraints when constructing the porous networks. Variable connectivity or geometrical restrictions may be allowed for.

2.4.1. Analytical expressions for sorption domain complexions

Analytical expressions describing the states of porous entities (filled with liquid or vapor) during diverse sorption processes have been previously established [11,12]. In these expressions $\theta_S(R)$ and $\theta_B(R)$ represent, respectively, the fraction of sites or bonds of size R that are filled with capillary condensate at a particular R_c. The overall degrees of filling of sites and bonds are then:

$$\theta_S = \int_0^\infty \theta_S(R) F_S(R)\,dR;$$
$$\theta_B = \int_0^\infty \theta_B(R) F_B(R)\,dR \quad (9)$$

In order to establish the particular sorption expressions, geometries have to be assigned to sites and bonds. In this work sites will be considered as hollow spheres and bonds as hollow cylinders open at both ends. Therefore, sites have several poles at which bonds are connected to them. Furthermore, the connectivity of the network C will be assumed constant. All the following equations are mean field or Bragg–Williams approximations. Analytical expressions for scanning curves of an order higher than one are less accurate because of an extended application of the mean field approximation and will not be dealt with in this work.

2.4.1.1. BA curve. Bonds, conceived as hollow cylinders, can fill in two ways. Independently if the bond radius is smaller than or equal to $R_c/2$, through a mechanism described by Everett and Haynes [10], or assistedly when one of its two delimiting sites becomes filled with condensate [13]. Domain complexions for bonds, $\theta_B(R)$, along the *BA* curve are then:

$$\theta_B(R) = \begin{cases} 1 & R \le \dfrac{R_c}{2} \\ [1-(1-J)^2] & \text{for } \dfrac{R_c}{2} < R \le R_l \\ 0 & R > R_c \end{cases} \quad (10)$$

where J is the probability that a bond being invaded by condensate in an assisted manner from a delimiting site, and for the case when $\Omega = 0$, J is given by

$$J = I^{C-1} S(R_c) \quad (11)$$

where, I represents the probability that a neighboring bond (not the incumbent one but any of the remaining $C-1$ bonds linked to this delimiting site), be already filled by condensate in an independent or assisted way:

$$I = B\left(\frac{R_c}{2}\right) + \left[1 - B\left(\frac{R_c}{2}\right)\right] J \quad (12)$$

So that all bonds with $R \le R_c/2$ will be completely filled with condensate and those with $R > R_c/2$ may be filled or not depending on the topology of the network and state of the system.

Correspondingly, domain complexion expressions for sites along the *BA* curve are

$$\theta_S(R) = \begin{cases} I^C + CI^{C-1}(1-I) & \text{for } R \le R_c \\ 0 & R > R_c \end{cases} \quad (13)$$

These expressions arise since a site can be filled with condensate when C or at least $C-1$ of its delimiting bonds have been invaded by condensate [13]. In this latter case the liquid–gas interface will proceed into the remaining empty bond causing its assisted filling with condensate.

2.4.1.2. BD curve. Domain complexions for sites during this boundary process are given by the expressions:

$$\theta_S(R) = \begin{cases} (1-K)^C & \text{for } R \ge R_c \\ 1 & R < R_c \end{cases} \quad (14)$$

K is the percolation probability that vapor invades the site, wherein two conditions are comprised: (a) the site should be large enough ($R \ge R_c$), and (b) there should exist a continuous trajectory to the bulk vapor phase from the site in question. K is then given for $\Omega = 0$ by

$$K = [1 - B(R_c)][1 - (1-K)^{C-1}] \quad (15)$$

For bonds, $\theta_B(R)$ is given by

$$\theta_B(R) = \begin{cases} (1-L)^2 & \text{for } R \geq R_c \\ 1 & R < R_c \end{cases} \quad (16)$$

L being the probability of vapor invading the bond, for $\Omega = 0$ this quantity becomes

$$L = 1 - \{B(R_c) + [1 - B(R_c)](1-L)\}^{C-1} \quad (17)$$

This expression for L arises from the fact that a bond will be invaded by vapor if (1) it is larger than R_c, and (2) there is a continuous path to the vapor phase through any one of the remaining $C-1$ bonds linked to the site delimiting the bond in question.

2.4.1.3. PA curves. Conditions at the reversal point on the *BD* curve are marked with an asterisk; $\theta_S^*(R)$ then being the degree of filling of a site of size R at this point. Domain expressions for sites are given by

$$\theta_S(R) = \begin{cases} \theta_S^*(R) + [(1-\theta_S^*(R)][I_{PA}^C + C I_{PA}^{C-1}(1 - I_{PA})] \\ \theta_S^*(R) \end{cases} \quad \text{for } \begin{matrix} R \leq R_c \\ R > R_c \end{matrix} \quad (18)$$

Whilst for bonds we have

$$\theta_B(R) = \begin{cases} 1 \\ \theta_B^*(R) + [(1-\theta_B^*(R)][1 - (1 - J_{PA})^2] \end{cases} \quad \text{for } \begin{matrix} R_u \geq R \\ R_u < R \leq R_c \end{matrix} \quad (19)$$

R_u being either R_c^* or $R_c/2$ whichever is larger, and in the case when $\Omega = 0$, J_{PA} and I_{PA} are given by

$$J_{PA} = I_{PA}^{C-1} S(R_c) \quad (20)$$

$$I_{PA} = B(R_u) + (1 - B(R_u)[\theta_B^*(R) + (1 - \theta_B^*(R) J_{PA}] \quad (21)$$

2.4.1.4. PD curves. The treatment is similar to the *BD* curve. For sites the degree of filling with condensate is

$$\theta_S(R) = \begin{cases} 0 & \text{for } R > R_c^* \\ \theta_S^*(R)(1 - K_{PD})^C & R_c^* \geq R \end{cases} \quad (22)$$

$\theta_S^*(R)$ being the degree of filling of a site R with condensate at the point of reversal and K_{PD} given by

$$K_{PD} = \frac{\theta_B^*(R_B)}{\theta_B^*}[1 - B(R_c)[1 - (1 - K_{PD})^{C-1}] \quad (23)$$

And for bonds

$$\theta_B(R) = \begin{cases} \theta_B^*(R)(1 - L_{PD})^2 & R_c^* \geq R \geq R_c \\ \theta_B^*(R) & \text{for } R_c > R > R_l \\ 1 & R \leq R_l \end{cases} \quad (24)$$

where R_l may be $R_c^*/2$ or R_c, depending on which is the smallest. L_{PD} is expressed as

$$L_{PD} = 1 - S(R_c^*) \times \left\{ \frac{B(R_l) + [B(R_c) - B(R_l)]\theta_B^*(R_l) + [1 - B(R_c)]\theta_B^*(R)(1 - L_{PD})}{\theta_B^*} \right\}^{C-1} \quad (25)$$

3. Results and discussion

3.1. Construction of porous networks by a Monte Carlo method

The strategy to be used in this work in order to ascertain the validity or contravention of the *ISDT* theorems in the case of sorption phenomena occurring in non-independent porous networks, is as follows. Heterogeneous three-dimensional porous networks (heterogeneous in the sense of having pores of different sizes subjected to some geometrical restrictions) consisting of a given number of void elements and constructed according to the premises of the *DSBM*, will be used to model non-independent domain substrata. The required twofold distribution for constructing the porous networks will be chosen as a double Gaussian, with no overlap between the site and bonds functions ($\Omega = 0$). The networks will be regular cubic 3-D lattices (i.e. with a constant connectivity of 6) with a constant node to node distance equal to 1.1 times the diameter of the largest site; sites will be allocated at the nodes of the network. Bonds will be connected in between the sites in such a way as to concurrently fulfill two conditions: (1) to be smaller than the site and (2) to avoid any interference with another neighboring

bond. This last condition is a geometrical restriction meaning that two orthogonal bonds R_{B1} and R_{B2} could be connected to a site of size R_S if only the following condition is fulfilled:

$$R_S \geq \sqrt{R_{B1}^2 + R_{B2}^2} \quad (26)$$

3.2. Simulation of sorption phenomena within selected substrata

To determine the incumbent sorption process of an adsorptive in contact with the simulated porous networks, it is necessary to take into account some specific criteria that are adequate for the filling of a pore with condensate or with vapor during an ascending or descending process, respectively [11–13]. These criteria are included ab initio in the calculating sorption program and are related to: (1) the critical conditions imposed by the Kelvin equation through a radius of curvature $R_{c,}$ for a phase transition to occur in a porous entity of a given geometry, and (2) to the sorptive cooperative phenomena that arise between neighboring elements depending on the states (empty or filled with condensate or vapor) of the porous entities involved in the process. We recognize the importance of the multilayer adsorbed film existing in pore entities, since the thickness of this film will indeed influence the conditions at which phase transitions occur in the pores. The effect of the adsorbed film will not be included in this work for the sake of simplicity. Furthermore, if we think that our simulated networks have sufficiently large pore sizes, then the effect of the adsorbed film may be negligible.

Specifically, for condensation and evaporation to occur in sites and bonds, requirements are as follows:

- Condensation of the adsorptive inside a vapor-filled bond (assumed as a hollow cylinder open at both ends) can occur in two possible ways: (1) by an *independent* filling, when half the value of the present critical radius of curvature ($R_c/2$) is equal to the pore radius; (2) by an *assisted* filling when a liquid–gas meniscus invades a bond (of a radius lesser than R_c but larger than $R_c/2$) from at least one of its two neighboring sites. In this latter case the bond is liquid filled ahead of the R_c value at which it would have occurred if the void were isolated; condensation has already proceeded in the site and pursued to the bond in question.
- Condensation in a site (assumed as a hollow sphere connected to neighboring homologous sites through C bonds) will occur in the following way. Besides the requirement to have a radius smaller than R_c, a site will be completely invaded if only C or at least $C-1$ of their bonds are already filled with condensate. This guarantees the formation and advancement of a continuous meniscus towards: (1) the center of the site (for the case of C liquid-filled bonds) or (2) to the remaining empty bond (for the case of $C-1$ filled bonds). In this latter case the liquid front continues its advancement into the remaining empty bond, invading it completely with condensate (i.e. an assisted bond filling occurs).
- Evaporation from a site or a bond requires two conditions to be concurrently satisfied. First that the radius of the element be larger than R_c and second the existence of a continuous vapor trajectory from the pore to the bulk vapor phase.

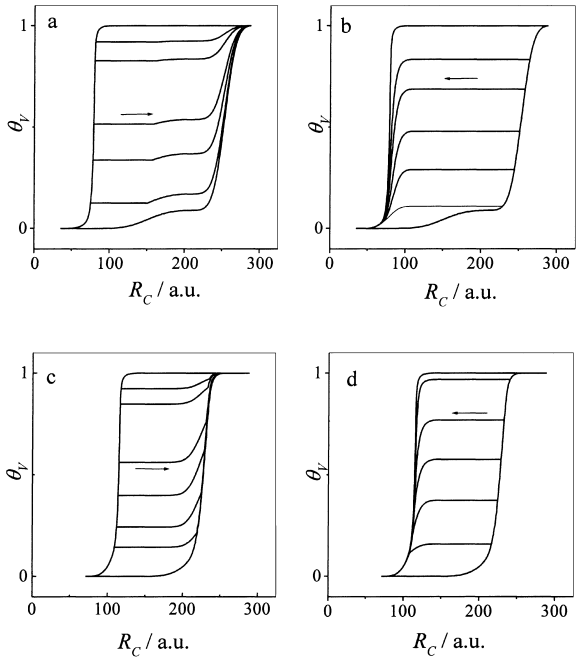

Fig. 3. Ascertainment of Theorems 1 and 2 of the *ISDT*, in networks constructed by Monte Carlo methods: (a) *PA* curves for Network 1; (b) *PD* curves for Network 1; (c) *PA* curves for Network 2; and (d) *PD* curves for Network 2.

In this work, the sorption curves calculated through the Monte Carlo method will be derived assuming that both sites and bonds contribute to the sorbed volume. The sorption isotherms then will be plotted in terms of R_c versus $\theta_{v,}$ the number fraction of voids filled with capillary condensate.

Finally, sometimes justification or contravention of some of the theorems advanced by the *ISDT* will also be made through the use of probabilistic expressions describing *BA*, *BD*, *PA* and *PD* sorption processes and that have been derived elsewhere [11,12].

3.3. Assessment of the ISDT theorems from the DSBM non independent pore domain point of view

Cubic porous networks with $C = 6$ and consisting of $80 \times 80 \times 80$ sites and its corresponding $3 \times 80 \times 80 \times 80$ bonds, are generated by a Monte Carlo procedure previously described in [8,14]. Two Gaussian distributions have been used in this work as site and bond input functions, their parameters are as follows:

Network 1. Mean size for bonds, $\overline{R}_B = 72$ a.u. (a.u. arbitrary units), mean size for sites, $\overline{R}_S = 252$ a.u., standard deviation for sites and bonds, $\sigma_B = \sigma_S = 12$ a.u.

Network 2. Mean size for bonds, $\overline{R}_B = 108$ a.u., mean size for sites, $\overline{R}_S = 216$ a.u., standard deviation for sites and bonds, $\sigma_B = \sigma_S = 12$ a.u.

These networks have been chosen to exemplify the appropriateness of the *ISDT* theorems in the case of non-independent domains because of the following reasons.

Network 1 corresponds to a type I in the *DSBM* classification [11] with $\Omega = 0$. This means that the diameter of the largest bond is lesser than the radius of the smallest site. This causes that condensation in

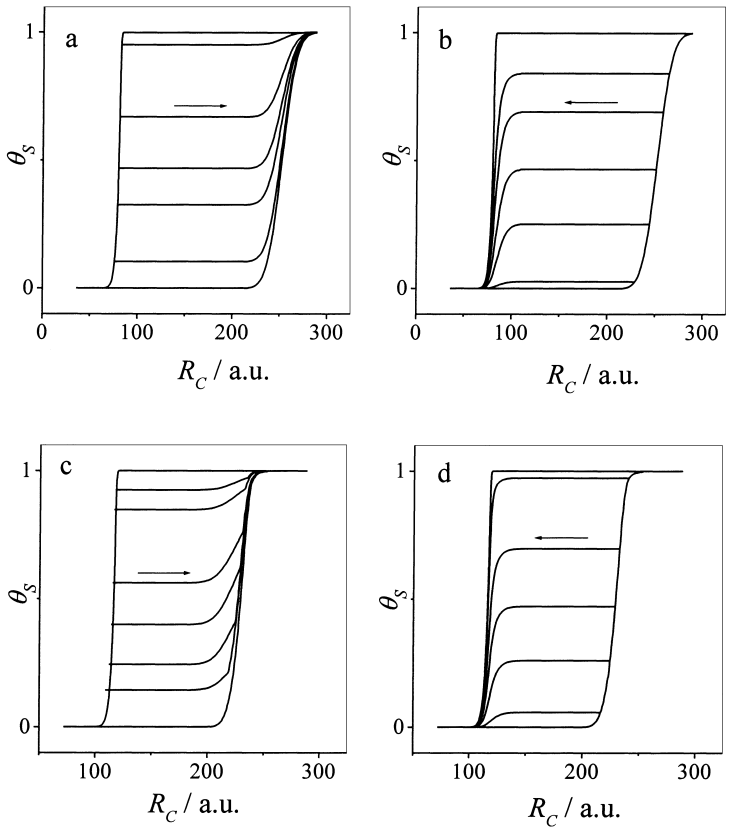

Fig. 4. Ascertainment of Theorems 1 and 2 of the *ISDT*, in networks constructed by analytical equations: (a) *PA* curves for Network 1; (b) *PD* curves for Network 1; (c) *PA* curves for Network 2; and (d) *PD* curves for Network 2.

both pores and bonds occur independently; bonds will be filled first in a sequential manner from the smallest to the largest one followed by sites in the same sequential fashion. Bonds acting as stoppers, on the other hand, will control evaporation and a percolative invasion by vapor will be expected in this type of structures. The behavior of this network will resemble that observed in independent domains for the cases of *BA* and *PA* curves. Therefore, the interest of studying this type of substrate resides in proving or refuting the latter assertion. Conversely, descending processes should be expected to markedly differ from the behavior shown by independent domains.

Network 2 corresponds to a type II of the *DSBM* classification [11]. In this substrate, there arise cooperative phenomena during both ascending and descending processes. The sorption properties of this network will divert from those of independent domains and the difference will be more accentuated than for Network 1. Besides geometrical restrictions imply an extra degree of correlation between pore elements in this network. In fact there exists some preference in having large sites surrounded by large bonds and small sites to be connected to small bonds. This is called a size segregation effect and influences very much the occurrence of capillary phenomena within substrata of this kind.

In brief, Network 2 is expected to show farther deviations than Network 1 with respect to the fulfillment of the theorems supplied by the *ISDT* when ascending processes are involved.

3.3.1. Specific results on the fulfillment or contravention of ISDT theorems in non-independent domains

3.3.1.1. Theorems 1 and 2. Simulated *PD* and *PA* curves for Networks 1 and 2 are presented in Figs. 3 and 4. On the one hand, Theorem 2 is fulfilled in the

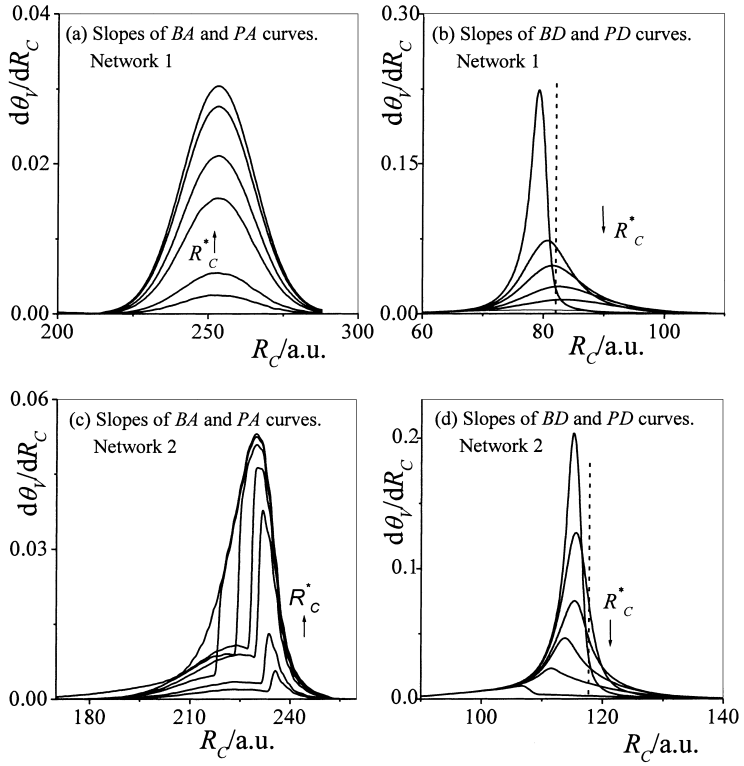

Fig. 5. Ascertainment of Theorems 3a and 3b of the *ISDT*, in networks constructed by Monte Carlo methods. Slopes of primary curves compared to those of boundary ones: (a) and (c) boundary and *PA* curves for Networks 1and 2, respectively; (b) and (d) boundary and *PD* curves for Networks 1 and 2, respectively. Dashed lines indicate the values of R_c at which $B(R_c) = (C-2)/(C-1)$ for descending curves.

case of Network 1 since both the *PD* and *PA* curves are asymptotic to the points of inception and conclusion of the *HL*, respectively. On the other hand, fulfillment of Theorem 1 is not complete in the case of Network 2, since although the *PA* curves practically intersect the *BA* curve before reaching the point of closure of the *HL*, the *PD* curves are in contrast asymptotic to the inception point. The same conclusions are reached when using the probabilistic equations that allow the tracing of *PD* and *PA* curves, Theorem 2 is satisfied for Network 1 in the way of a series of asymptotic *PA* and *PD* curves. In the case of network 2 again *PA* curves practically intersect the *BA* curve (see Fig. 4), something that is not so for *PD* curves since these approach the *BD* curve asymptotically.

An explanation for this behavior in the case of Monte Carlo calculations, is that Network 1 possesses pore entities that are no correlated at all: first bonds and sites afterwards fill gradually, according to their sizes along the *BA* curve. In the case of Network 2 there is already certain interdependency between the filling of neighboring entities. The *PA* curves practically reach the *BA* curve when $R_c \approx 2R_c^*$, thus the filling of pore entities change from a gradual to a more intense one, once the independent filling of bonds is reassumed. It can be said as Everett [3] stated before that a broad distribution of domain properties redounds in asymptotic sorption curves (i.e. Network 1) and a narrower distribution redounds in *SC* intersecting the boundary ones before the closure and inception points (i.e. Network 2).

3.3.1.2. Theorems 3a and 3b. For Networks 1 and 2 (Fig. 5a and c, respectively) show the evolution of the slopes of a series of *PA* curves $d\theta_S/dR_c$ in terms of R_c. Fig. 5b and d represent the same slope evolution for a series of *PD* curves. From these graphs it can be seen that the initial slopes of either *PA* or *PD*

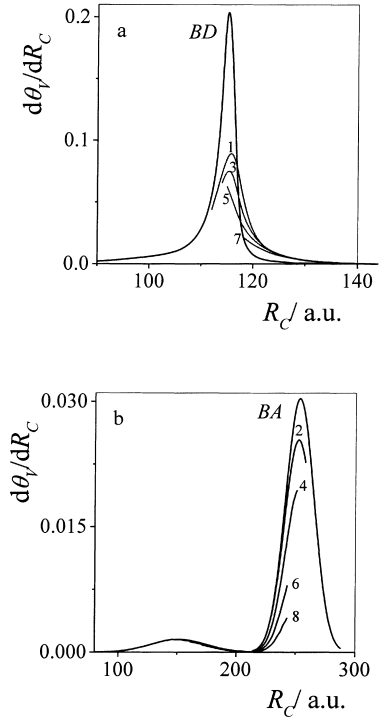

Fig. 6. (a) Slopes of descending scanning curves of different orders — 1: primary, 3: tertiary, 5: quinquenary, 7: septenary, Network 2. (b) Slopes of ascending scanning curves of different orders — 2: secondary, 4: quaternary, 6: sexenary, 8: octonary, Network 1.

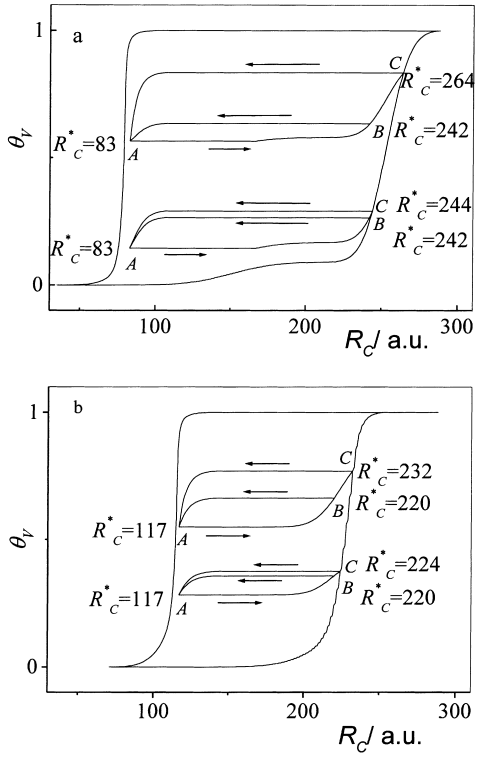

Fig. 7. Ascertainment of Theorem 4 of the *ISDT*. Loops *AB* are traced between the same limits for both (a) Network 1 and (b) Network 2.

curves are zero, thus confirming the expectations of Theorem 3a.

With respect to Theorem 3b, in the case of Network 1, it can be observed the slope of the *BA* curve is always higher than the slopes of its lower order *PA* curves (see Figs. 5a and 6b). Theorem 3b is faithfully fulfilled, thus once more reflecting the independent liquid filling of pore cavities according to size in this type of network.

In the case of Network 2 it can be observed in Fig. 5c that the slope of the *BA* curve is higher than the slopes of its lower order *PA* curves for most part of the R_c interval except at low values of this parameter. There is a maximum slope for *PA* curves at intermediate values of R_c. This maximum occurs when $R_c \approx 2R_c^*$, at which point the independent bond filling reassumes after evaporation had been interrupted at the inversion point. The smaller initial slope values (i.e. at low R_c) are due to the filling of sites that are surrounded by $C-1$ already filled bonds. Once these sites are occupied there is a discontinuity since the filling proceeds gradually until reaching a percolation threshold when $R_c \approx 2R_c^*$, after which the filling is continued again but in a more tenuous way. The discontinuity above mentioned occurs when a critical proportion of bonds are filled with condensate, causing the sudden liquid invasion of sites of sizes smaller than R_c.

Thus, for Network 1 Theorems 3a and 3b are completely fulfilled in the case of *PA* curves; however this is not true for *PD* curves. In this case, the evaporation threshold appears when the blockage to the entrance of the vapor phase, imposed by liquid-filled elements,

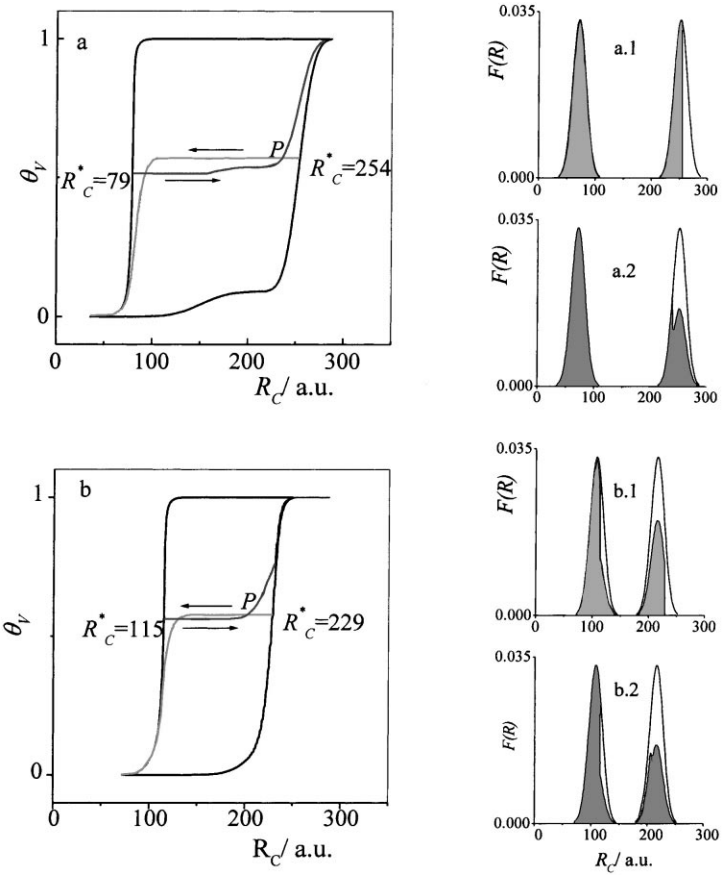

Fig. 8. Ascertainment of Theorem 6 of the *ISDT*. (a) Crossing of *PD* and *PA* curves at point *P* for Network 1. (b) Crossing of *PD* and *PA* curves at point *P* for Network 2 (a.1 and b.1). Complexion diagrams for the *PD* curves (a.2 and b.2). Complexion diagrams for the *PA* curves.

is removed. Thus, before the evaporation threshold appears, there is a plateau region of variable extension depending on the location and order of the descending curve. For either Network 1 or Network 2 Theorem 3b is not but partially fulfilled over the whole R_c range (Fig. 5b and d). At large R_c values the slope of a higher order *PD* curve is steeper than the slope of the *BD* curve (see Fig. 6a), but the converse is true at lower R_c values. At high R_c's, the free vapor path required for a pore to be emptied of condensate, is indeed harder guaranteed for the case of the *BD* curve than for any of the *PD* curves. This happens since desorption along the *BD* curve at high R_c values, i.e. at high relative pressures, starts from a completely liquid-filled system. This is not the case of *SC*, where the reversal point corresponds to a partially liquid-filled structure. With respect to the extension of the plateau the percolation threshold for vapor invasion [15] is given at a R_c value such that $B(R_c) = (C-2)/(C-1)$, this is approximately fulfilled by the *BD* curve.

3.3.1.3. Theorem 4. This theorem is fulfilled by both Networks 1 and 2 in the sense that if the system is at state *A* ($R_c = R_{CA}$), afterwards taken to state *B* (R_{CB}), and when R_c is reversed to R_{CA} again, then the system will return to state *A*. Fig. 7a and b show the subsidiary loops obtained through this procedure. However Theorem 4 is not fulfilled in the sense that any oscillation of R_c between two given limits R_{CA} and R_{CB}, should lead to a loop of constant shape independently of the position of state *A* in the loop (compare the two subsidiary loops in Fig. 7a and b). The difference in shape between subsidiary loops may be ascribed to the different domain complexions existing at the different *A* points at which the subsidiary loops have begun: the intensities of cooperative phenomena during adsorption and desorption and thus the shape of a subsidiary loop depend on the state of the system at point *A*.

3.3.1.4. Theorem 5. This theorem is completely fulfilled for both Networks 1 and 2. Fig. 7a and b show the evolution of a system for a secondary ascending scanning curve and for a system that has undergone first a loop from the same starting point that the secondary curve and then reassumed its movement. It is from point *B* that the two trajectories moves up to point *C*, thus fulfilling the expectations of Theorem 5. The cyclical process *BAB* restores the system to the domain complexion state that existed before of the start of the subsidiary loop.

3.3.1.5. Theorem 6. This theorem is appropriate for Networks 1 and 2. Fig. 8a and b show the departures of *PA* and *PD* curves after coinciding at some point *P*; complexion diagrams are shown for each curve at the intersection point. The system acquires different domain complexions depending on the route followed to reach *P*, so that different approaches to this point result in different departing trajectories when the system moves away from *P*.

3.3.1.6. Theorem 7. Once again this theorem is faithfully complied by Networks 1 and 2. The spiral trajectories shown in Fig. 9a and b are graphical proofs of the validity of this theorem in the case of interacting pore domains.

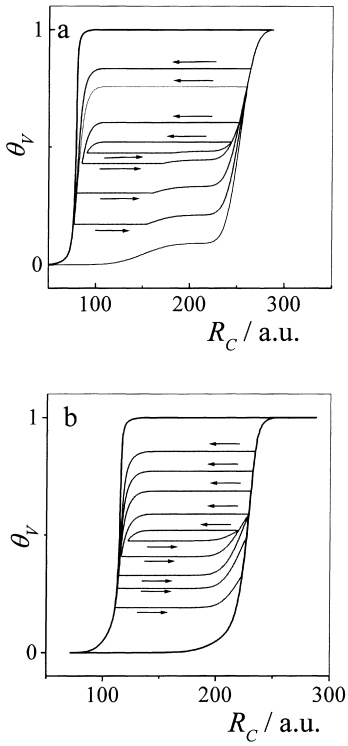

Fig. 9. Ascertainment of Theorem 7. Spiral trajectories for (a) Network 1 and (b) Network 2.

4. Conclusions

On the one hand Theorems 1, 2, 3a, 3b and 4 of the *ISDT* are of a limited qualitative validity, for the case of porous structures constituted by non-independent pore domains, depending on the porous topology of the network: the lesser correlated the pore elements are, the greater is the accordance with the predictions of the *ISDT*. For the case of a network type I in the DSBM classification, all theorems involving ascending curves are completely fulfilled.

On the other hand, Theorems 5–7 are indeed qualitatively valid for sorption processes in both independent and non-independent structures no matter the topological nature of the porous network.

An additional observation is that percolation thresholds can be detected, in general, for ascending and descending processes in the case of non-independent domains. Percolation thresholds for ascending processes only occur for the case of correlated structures but not for type I structures.

In this work, substrata have been assumed to be lattices of constant connectivity, it would be interesting to see what happens with a network of variable connectivity with respect to the theorems of the *ISDT*.

Acknowledgements

Thanks are due for the financial support: (1) to CONACyT (México), Project “Medios Porosos, Superficies, Procesos Capilares y de Adsorción”, No. 28416E (1998); (2) to FOMES (SEP, México) Project “Medios Porosos y Superficies: Preparación y Caracterización”, No. 98-35-21; and (3) to CONACyT-SECYT (Argentina): “Medios Complejos y Físicoquímica de Superficies (2000)”.

References

[1] D.H. Everett, W.I. Whitton, Trans. Faraday Soc. 48 (1952) 749.
[2] D.H. Everett, F.W. Smith, Trans. Faraday Soc. 50 (1954) 187.
[3] D.H. Everett, Trans. Faraday Soc. 50 (1954) 1077.
[4] D.H. Everett, F.W. Smith, Trans. Faraday Soc. 51 (1955) 1551.
[5] D.H. Everett, in: E.A. Flood (Ed.), The Solid–Gas Interface, Vol. 2, Marcel Dekker, New York, 1967, Chapter 36, p. 1055.
[6] V. Mayagoitia, M.J. Cruz, F. Rojas, J. Chem. Soc., Faraday Trans. 1 85 (8) (1989) 2071.
[7] V. Mayagoitia, F. Rojas, I. Kornhauser, H. Pérez-Aguilar, Langmuir 13 (5) (1997) 1327.
[8] A.J. Ramírez-Cuesta, S. Cordero, F. Rojas, R.J. Faccio, J.L. Riccardo, J. Porous Mater. 8 (1) 2001.
[9] V. Mayagoitia, F. Rojas, I. Kornhauser, G. Zgrablich, R.J. Faccio, B. Gilot, C. Guiglion, Langmuir 12 (1) (1996) 1207.
[10] D.H. Everett, J.M. Haynes, J. Coll. Int. Sci. 38 (1972) 125.
[11] V. Mayagoitia, F. Rojas, I. Kornhauser, J. Chem. Soc., Faraday Trans. 1 84 (1988) 785.
[12] V. Mayagoitia, B. Gilot, F. Rojas, I. Kornhauser, J. Chem. Soc., Faraday Trans. 1 84 (1988) 801.
[13] V. Mayagoitia, F. Rojas, I. Kornhauser, J. Chem. Soc., Faraday Trans. 1 81 (1985) 2931.
[14] M.J. Cruz, V. Mayagoitia, F. Rojas, J. Chem Soc., Faraday Trans. 1 85 (8) (1989) 2079.
[15] F. Rojas, I. Kornhauser, J. Salmones, S. Cordero, J.M. Esparza, C. Felipe, in: F. Meunier (Ed.), Fundamentals of Adsorption, Vol. 6, Elsevier, Paris, 1998, p. 327.